JOURNAL OF PROPULSION AND POWER
Vol. 27, No. 4, July–August 2011

Streamwise Evolution of Loss in a Shrouded Axial Compressor Cascade Passage

J. W. Kim* and S. J. Song†
Seoul National University, Seoul 151-742, Republic of Korea
and
T. Kim‡
University of the Witwatersrand, Johannesburg 2050, South Africa

DOI: 10.2514/1.B34006

Streamwise evolution of blade passage flows, including loss and flow turning, has been characterized experimentally and numerically. Experimentally, to simulate rotation effects in a shrouded axial compressor linear cascade, the leakage flow in the shrouded seal cavity is artificially circulated through a secondary flow loop connecting both sidewalls of the shrouded cavity. The overall loss and deviation have been measured downstream of the stator blade row at the design point, and the results compare well with the data from a rotating environment. To gain further physical insights into how the passage flow near the blade/endwall surfaces behaves at the downstream cavity trench, numerical simulation has been conducted. Detailed flow data obtained from the experiment and numerical simulation consistently demonstrate that the loss is successively increased from the leading edge up to the upstream edge of the downstream cavity trench. As the mainstream passes over the downstream cavity trench, however, the loss is decreased as the high-loss fluids concentrated near the hub endwall are engulfed into the downstream cavity. Downstream of the blade row, the loss increases again due to the wakes from the trailing edge of the stator blade.

Nomenclature

C	=	blade true chord, m
c	=	mainstream velocity at $0.5C_x$ upstream from blade leading edge, m/s
C_x	=	blade axial chord, m
c_x	=	axial velocity component of mainstream, m/s
H	=	blade span, m
h	=	cavity depth, m
k_1	=	inlet blade angle, °
k_2	=	exit blade angle, °
P_1	=	total pressure at $0.5C_x$ upstream from blade leading edge, Pa
P_2	=	total pressure in traverse plane, Pa
p_1	=	static pressure at $0.5C_x$ upstream from blade leading edge, Pa
R_{hub}	=	hub radius, m
R_{tip}	=	tip radius, m
Re_C	=	Reynolds number based on blade true chord and mainstream velocity at test section inlet
S	=	blade pitch, m
U_{hub}	=	rotating hub speed, m/s
U_{tip}	=	rotor tip speed, m/s
v_y	=	tangential velocity component of leakage flow in seal cavity, m/s
x	=	axial direction
y	=	tangential direction
Y_p	=	loss coefficient [Eq. (1)]
z	=	radial direction
β_1	=	inlet flow angle, °
β_2	=	exit flow angle, °
δ	=	deviation [Eq. (2)], °
ε	=	seal clearance, m

I. Introduction

IN SHROUDED axial flow turbomachines, there are inevitable gaps between stationary and rotating components. The leakage flow through the gaps causes significant efficiency and aerodynamic performance degradation. Shrouding is one way of reducing the leakage flows through the gaps and improving structural integrity. When stator blades are shrouded, the hub ends of blades are connected to an annular ring, or the inner band, while the upper ends of blades are attached to the casing. Between the inner band and shrouded cavity endwall, a single or multiple seal-tooth assembly is often used to reduce the leakage flow rate through the shrouded cavity.

Figure 1 shows a schematic of an axial compressor stator blade shrouded at the hub with a single-tooth labyrinth seal. Because of the adverse axial pressure gradient across the stator blade row (along the x axis), the leakage flow is engulfed into the seal cavity through the downstream cavity trench. This leakage flow migrates from the downstream cavity region to the upstream cavity region across the seal, and then it rejoins the mainstream through the upstream cavity trench. Thus, the leakage flow interacts with the mainstream and affects the aerodynamic performance of a shrouded axial compressor.

Wisler [1] and Wisler et al. [2] observed that the leakage flow increases blockage and secondary flow mixing in the mainstream, resulting in increased loss in a low-speed research compressor (LSRC). Typically, 1% of the total mainstream mass flow rate leaks through for each percent of seal-clearance/blade span ratio [1]. Wellborn and Okiishi [3,4] found that the leakage flow spoiled the near-hub performance of the stator and altered exit flow conditions in multistage axial compressors. Furthermore, an efficiency degradation of 1% and a 3% penalty in the pressure rise for each percent increase in the seal-tooth clearance-to-blade height ratio were found. Similar trends have been predicted numerically by Heidegger et al. [5].

Received 8 May 2010; revision received 2 January 2011; accepted for publication 4 January 2011.

*Graduate Research Assistant, School of Mechanical and Aerospace Engineering.
†Professor, School of Mechanical and Aerospace Engineering.
‡Associate Professor, School of Mechanical, Industrial, and Aeronautical Engineering.

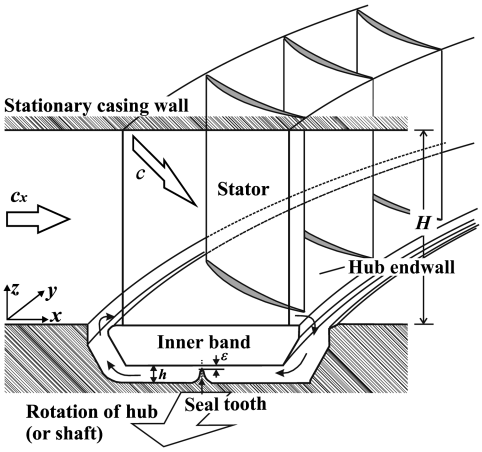

Fig. 1 Bird's eye view of the stator blade row with fully shrouded cavity.

Wellborn and Okiishi [4] also observed that the low momentum fluids moved from the blade pressure side to the blade suction side due to the cross-passage pressure gradient near the hub endwall. These fluids collect on the suction surface of the stator blade, and then they lead to suction side hub corner separation, which subsequently increases the hub endwall loss. Thus, even though the injected leakage flow through the upstream cavity is confined to the near-hub endwall region, it has a global effect on the compressor's aerodynamic performance.

Typical cascade experiments do not involve rotating blades, and researchers have attempted to simulate the rotation effect in linear cascades by employing moving endwalls. For example, Yaras and Sjolander [6] and Yaras et al. [7] examined the effect of the simulated relative motion in a linear cascade by using a moving-belt tip wall. Palafox et al. [8] conducted particle image velocimetry measurements of overtip leakage flows and associated endwall flows in the blade passage in a large-scale linear cascade with a moving tip wall. Krishnababu et al. [9] performed a numerical study on the effects of relative casing motion on the tip leakage flow and heat transfer characteristics. However, these studies have been limited to unshrouded turbine cascades, focusing on the tip leakage flows.

In shrouded compressor blades, the tangential velocity of the leakage flow within the seal cavity is determined by the combination of the tangential momentum of the passage flow entering the seal cavity via the downstream trench and the relative motion of the rotating hub endwall. Demargne and Longley [10] examined the effects of leakage flow tangential velocity on the performance of a linear cascade. They used a linear compressor cascade with separate upstream (used for blowing) and downstream (used for suction) slots to simulate seal effects. They found reductions of the overall blockage and loss with increasing leakage flow tangential velocity. By employing the same method, de la Rosa Blanco et al. [11] investigated the effects of the leakage flow on near-hub endwall flows in a turbine cascade with only an upstream slot.

Despite such efforts, the effects of the existence of an actual seal cavity on the performance of shrouded compressor blades have not yet been examined in a cascade environment. Furthermore, detailed information about the evolution of loss near the hub in the shrouded stator blade passage is still lacking. Therefore, the objectives of this study are 1) to present and validate a newly developed linear shrouded compressor cascade with an actual seal cavity that employs a secondary flow loop to vary the leakage flow tangential velocity in the seal cavity, and 2) to use the validated compressor cascade to investigate the detailed streamwise evolution of loss within a shrouded stator blade passage.

II. Experimental Setup

A. Test Facility

A new linear cascade facility with a full shrouded seal cavity and a secondary closed loop for leakage flow has been newly designed and built. The facility consists of an open-type compressor cascade with a seal cavity and a secondary closed flow loop for the leakage flow. The test section is schematically illustrated in Fig. 2. Air at ambient conditions is drawn by a centrifugal fan and then passes through a settling chamber and a contraction section (not shown in Fig. 2). The test section contains six shrouded compressor stator blades and a single seal-tooth labyrinth seal. The secondary flow loop is installed at both sidewalls of the seal cavity to circulate the leakage flow. Inside the secondary flow loop, a controllable fan is used to adjust the leakage flow tangential velocity in the seal cavity [12–14].

The use of a single seal tooth and a flat inner band is a simplification of actual compressors. However, it is believed that an understanding of the flow kinematics in this simple configuration would be a first step toward understanding the aerodynamic performance found in more complicated geometries. Stator A blade geometry at the midspan of General Electric's LSRC has been used to fabricate two-dimensional blades [15]. Parameters of the blades and the test section are listed in Table 1. During the tests, the mainstream velocity measured at $x/C_x = -0.5$ from the blade leading edge (LE) is 20 m/s. Consequently, the Reynolds number based on the blade true chord is $Re_C = 2.6 \times 10^5$.

B. Determination of Leakage Flow Tangential Velocity

Given $c = 20$ m/s, the inlet flow angle of $\beta_1 = 47.5°$, and the design flow coefficient of General Electric's LSRC (with stator A), c_x/U_{tip}, of 0.407 [15], the axial velocity is 13 m/s and U_{tip} is 33 m/s. According to Wellborn and Okiishi [3], area averaging of the leakage flow tangential velocity data in both upstream and downstream cavities yields a leakage flow tangential velocity having about 35% of the blade hub speed, i.e., $v_y/U_{\text{hub}} \sim 0.35$. As the LSRC's hub-to-tip ratio of the stator blade is $R_{\text{hub}}/R_{\text{tip}} = 0.85$, the hub speed is then estimated to be $U_{\text{hub}} = 28$ m/s. Therefore, in

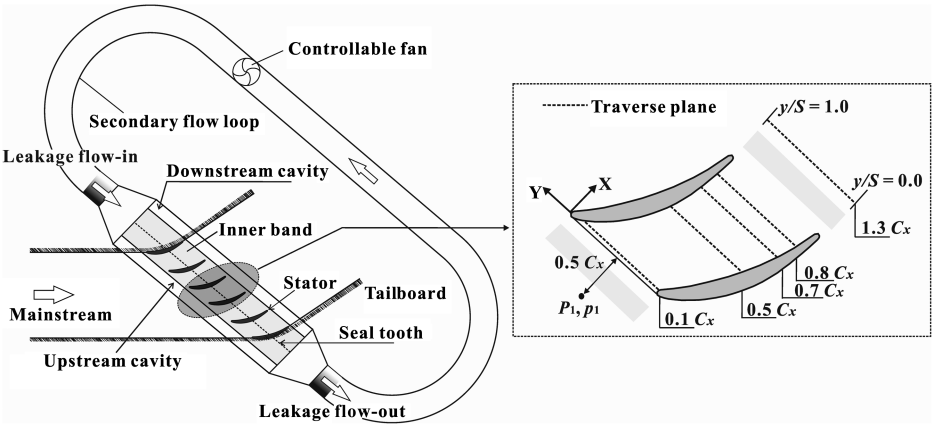

Fig. 2 Schematic of linear cascade test section with fully shrouded seal cavity and measurement locations in midpassage of the cascade facility.

Table 1 Parameters of stator blade and test section

Test parameter	Value
Blade true chord C, mm	200
Blade axial chord C_x, mm	168.6
Blade pitch S, mm	126.6
Blade span H, mm	196
Solidity C/S	1.58
Aspect ratio H/C	0.98
Inlet blade angle k_1, °	53.5
Exit blade angle k_2, °	14.8
Cavity depth h, mm	16
Seal-clearance ratio ε/H	0.01
Seal-clearance ratio ε/h	0.12

the present study, the leakage flow tangential velocity v_y has been set to be 9.8 m/s for the design point.

C. Instrumentation

Before experiments, cascade periodicity has been checked by monitoring the pitchwise static pressure variation. A single row of pressure taps across multiple passages has been placed on the casing endwall at $0.5C_x$ downstream from the blade trailing edge (TE). Two tailboards are attached to the sidewalls of the test section so that the pitchwise pressure distribution could be adjusted.

Measurement locations in the blade passage are illustrated in Fig. 2. To monitor the incoming mainstream velocity c, a pitot tube is positioned at $0.5C_x$ upstream from the blade LE. The leakage flow tangential velocity (which is measured by using another pitot tube placed at the cavity inlet of the cascade test section) can be adjusted to a desired value by the fan inserted in the secondary flow loop. To measure loss and deviation, a prismatic-type five-hole probe with an outer diameter of 3.1 mm is traversed at $x/C_x = 1.3$ from the blade LE. The total pressure and exit flow angles are obtained on a grid of 31 (over the entire span) times 21 (over one pitch) points. Measurement points are concentrated near the hub and tip endwall regions and in the blade wakes. In addition, the five-hole probe has been traversed at four selected axial chordwise locations, $x/C_x = 0.1$, 0.5, 0.7, and 0.8. The first measurement points on the blade suction and pressure surfaces and the hub endwall are located 5% blade pitch and 3% blade span off from the surfaces, respectively, due to the configuration of the (prismatic type) five-hole probe.

D. Data Reduction

To evaluate loss, the loss coefficient (Y_p) is defined as

$$Y_p = \frac{P_1 - P_2}{P_1 - p_1} \tag{1}$$

where P_2 is the measured total pressure in the traverse plane and P_1 and p_1 are the total and static pressures at $0.5C_x$ upstream from the LE of the stator blade, respectively. The Reynolds number Re_C is defined based on the blade true chord C and upstream mean velocity c at $0.5C_x$ upstream from the blade LE, and it is fixed to be $Re_C = 2.6 \times 10^5$ for all of the experiments. Deviation δ is measured using the same five-hole probe at the same downstream plane as the loss coefficient and is defined as

$$\delta = \beta_2 - k_2 \tag{2}$$

where β_2 and k_2 are the exit flow angle and exit blade angle, respectively. The measurement uncertainty associated with the loss coefficient Y_p is estimated to be within 2.7%, with a 95% confidence interval using the method of Coleman and Steele [16]. The error associated with deviation δ was found to be less than 0.5° with a 95% confidence interval.

III. Numerical Simulation

To obtain further physical insights into how the passage flow near the blade/endwall surfaces behaves at the downstream cavity trench and to complement the lacking of the measurement data points near the blade and endwall surfaces, computational fluid dynamics (CFD) have been conducted. Furthermore, the meshes were generated in ICEM CFD™ and then were exported to CFX™. The total number of the generated mesh cells was approximately 2.0×10^6. ANSYS CFX version 12.1 was used for the calculations. The Reynolds-averaged Navier–Stokes model was employed with shear stress transport k-ω turbulence model. The computational domain was extended from $1.0C_x$ upstream of the blade LE to $1.5C_x$ downstream of the blade TE in the axial direction, as illustrated in Fig. 3. For inflow and outflow boundary conditions, the inlet velocity profile obtained from experiment and downstream ambient air pressure were imposed, respectively. To simulate the rotation effect for the numerical simulation, the boundary condition is adopted to a moving wall at the lower cavity endwall.

IV. Discussion of Results

A. Loss and Exit Flow Turning at Design Point

To characterize the cascade's aerodynamic performance, loss and deviation have been measured at $x/C_x = 1.3$. Span and pitchwise distributions of the loss and deviation at the design point are first considered. Figure 4 depicts the spanwise (vertical axis) and pitchwise (horizontal axis) distribution of loss Y_p contour for $v_y/U_{\text{hub}} = 0.35$ measured at $x/C_x = 1.3$ and $Re_C = 2.6 \times 10^5$. A wake region near the midspan of the stator, covering between 80 and 95% of the blade pitch, is observed experimentally. Regions of endwall loss, caused by suction side corner separation, are generated near the hub ($z/H = 0.0$) and tip ($z/H = 1.0$). Because of the egress of the leakage flow from the shrouded cavity through the upstream cavity trench, and the ingress of the leakage flow into the cavity through the downstream cavity trench, the high loss is concentrated near the hub endwall ($z/H = 0.0$), showing higher loss generation than that near the tip region ($z/H = 1.0$). The hub loss region reaches up to 30% of the blade span, and it is mostly concentrated near the blade suction side hub corner.

The observed loss contour is then mass averaged in the pitchwise direction, and results are plotted in Fig. 5a, exhibiting the spanwise distribution of the loss coefficient. Similar to the loss contour plot

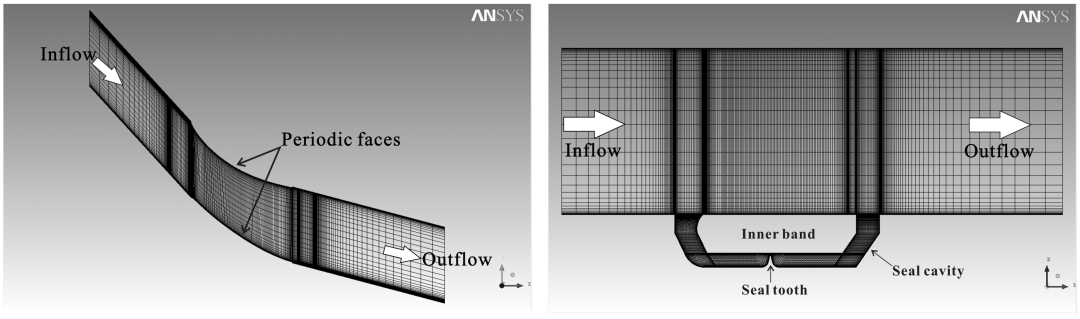

a) b)

Fig. 3 Computational flow domain and generated grid: a) plane view and b) side view.

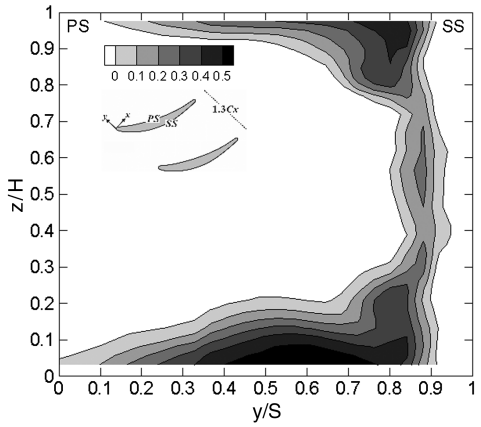

Fig. 4 Measured distribution of total pressure loss coefficient Y_p at $x/C_x = 1.3$ for the design point, $v_y/U_{\text{hub}} = 0.35$ (contour interval is 10% of inlet dynamic head).

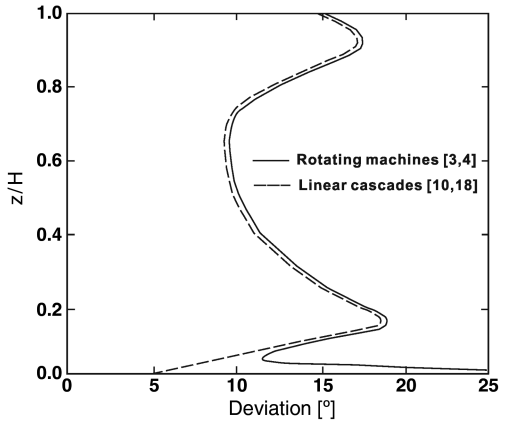

Fig. 6 Schematic of spanwise distributions of exit flow turning at the downstream of the compressor stator blade for rotating machines [3,4] and linear cascades [10,18].

(Fig. 4), the hub endwall loss region is wider in the spanwise direction than that of the tip region due to the seal cavity; thus, the radial extent of the hub endwall loss region spreads up to 30% of the blade span from the hub endwall. Furthermore, the loss coefficient at the midspan, having a value of $Y_p = 0.04$, is quantitatively consistent with the results obtained for the same blade by Wisler [17] in a rotating environment (i.e., LSRC). Finally, the numerically simulated data show good agreement with those experimentally measured, validating present numerical simulation.

The corresponding spanwise distribution of the deviation (mass averaged in the pitchwise direction) is plotted in Fig. 5b. For comparison, the pitchwise mass-averaged deviation at the midspan of the LSRC's stator A blade [17] is also included. The deviation data indicate a positive deviation (underturned) along the entire span, except near the tip region. At the midspan, the measured deviation from the current study is approximately $+6°$, showing good agreement with the measured midspan deviation of $+6.16°$ from the LSRC [17]. Moving toward the hub from midspan, the deviation is pronouncedly increased near the hub (e.g., $0.2 \leq z/H \leq 0.5$). It then decreases suddenly before increasing again in the vicinity of the hub. According to Wellborn and Okiishi [4], when the leakage flow tangential velocity in the upstream cavity trench is high enough to overcome the cross-passage pressure gradient, the lower momentum fluids collect on the pressure side of the stator blade as it travels downstream. Thus, the hub endwall flow is underturned at the downstream cavity trench. Consequently, the deviation near the hub is increased. In addition, the numerical simulation captures the spanwise details of the deviation quantitatively and qualitatively,

Before proceeding further, it is instructive to summarize the credibility of the data obtained from the newly developed shrouded axial compressor cascade. Figure 6 schematically shows the representative deviation patterns of a compressor stator blade row in both linear cascades and rotating rigs. In linear cascades, the deviation is successively decreased near the hub endwall from a maximum value at approximately $z/H \sim 0.15$ [10,18]. On the other hand, in a shrouded axial compressor (i.e., rotating rig), Wellborn and Okiishi [3,4] observed a sudden increase in deviation between the hub and 5% of the blade span. Thus, the new cascade with an actual seal (used in this study) can simulate rotational effects near the hub endwall in a stationary environment. The overall loss and exit flow turning distributions observed in the new linear cascade match the data from rotating rigs well, qualitatively and quantitatively.

B. Streamwise Evolution of Loss in a Blade Passage at the Design Point

In compressor cascades without a tip clearance, the suction side corner separation near the blade TE is one of the main factors influencing the loss generation in the blade passage. As the crossflow due to the pitchwise pressure gradient in the blade passage transports the low momentum fluids from the pressure side to the suction side of the blade near both tip and hub endwalls, high-loss fluids are successively collected near the TE of the blade suction side. This trend, combined with the adverse pressure gradient on the suction surface in the aft chord region, leads to boundary-layer separation on the suction surface near both endwalls. Consequently, the loss near the endwall is continuously increased as the mainstream flow convects along the blade passage. However, the situation is different for a shrouded compressor cascade with a seal cavity at the hub endwall.

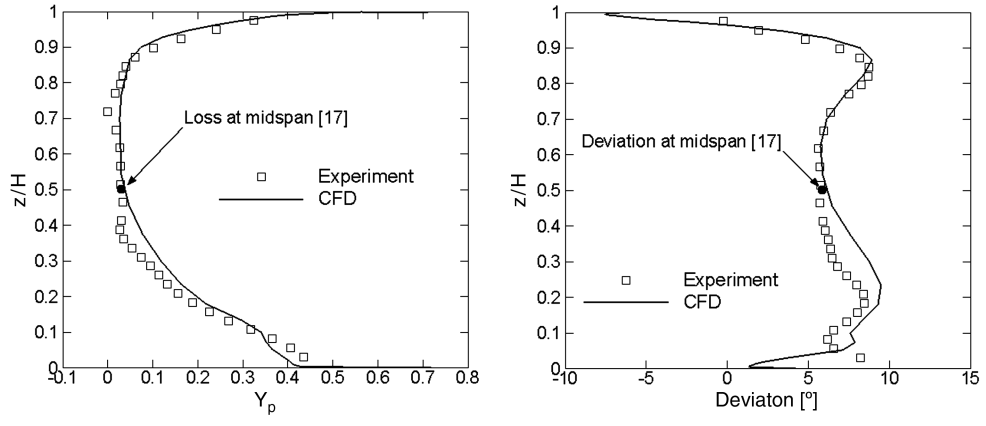

a) b)

Fig. 5 Spanwise distributions of measured and numerically simulated (CFD) pitchwise mass-averaged data at $x/C_x = 1.3$ for the design point, $v_y/U_{\text{hub}} = 0.35$: a) total pressure loss coefficient Y_p and b) deviation δ.

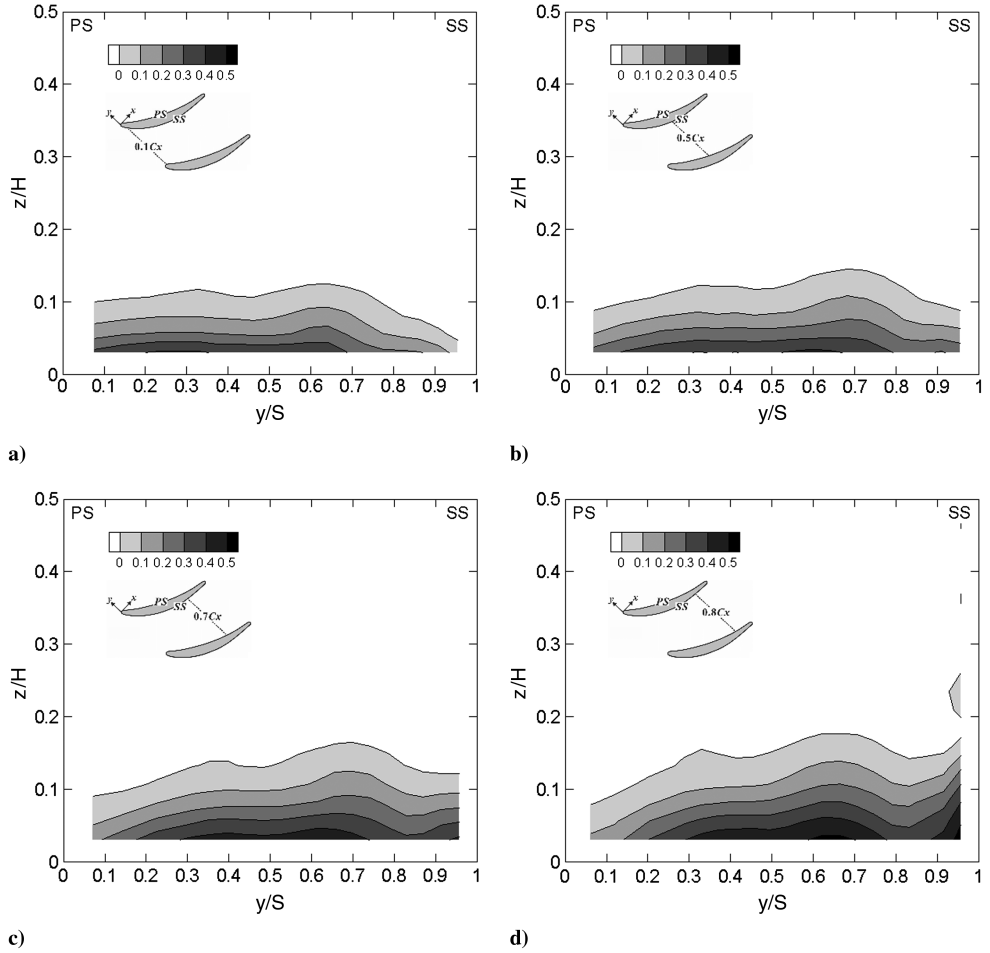

Fig. 7 Measured span and pitchwise distributions of loss coefficient in the passage at four selected axial chordwise locations for the design point, $v_y/U_{\mathrm{hub}} = 0.35$: x/C_x= a) 0.1, b) 0.5, c) 0.7, and d) 0.8.

In this section, loss and its evolution in the blade passage along the streamwise direction at the design point $v_y/U_{hub} = 0.35$ for $Re_C = 2.6 \times 10^5$ are considered. Figure 7 plots the contours of measured loss coefficient at four selected axial chordwise locations: $x/C_x = 0.1$, 0.5, 0.7, and 0.8. In Fig. 4, the loss generation near the hub region is shown to be more substantial than that near the tip region, due to the flow interaction between the mainstream and leakage flows at the both upstream and downstream cavity trenches. Previous studies [4,10] revealed that the leakage flow significantly affects the mainstream flow up to 40% span from the hub endwall downstream of the stator blade. Therefore, only the data from the inner 50% of the overall span are presented here. The contour interval is 10% of the inlet dynamic head.

At $x/C_x = 0.1$ (Fig. 7a), the loss region is radially spread up to about 10% of the blade span. Additionally, the high-loss region is spread up to 70% pitch of the blade from the blade pressure side. Farther downstream, at $x/C_x = 0.5$ and 0.7 (Figs. 7b and 7c), the high-loss region has moved toward the suction side but the radial extent has not changed much. The migration of the high-loss region toward the suction side represents the crossflow in the blade passage. Still farther downstream, at $x/C_x = 0.8$ (Fig. 7d), the high-loss region is concentrated in the hub suction side corner. The radial extent of the loss region is significantly increased. The increase in the high-loss region is due to the hub corner separation at the blade suction side.

To elaborate on the observed loss generation at each streamwise location, the loss coefficient below the midspan has been mass averaged at each chordwise location. Figure 8 shows that until the upstream edge of the downstream cavity trench, the total loss $\mathrm{CFD}_{\mathrm{whole}}$ is monotonically increased, followed by a decrease in the loss downstream of the downstream cavity trench. As the mainstream convects along the blade passage, the high-loss fluids are continuously collected near the blade suction side in the vicinity of the hub endwall due to the cross passage pressure gradient. Thus, the loss is successively increased up to the upstream edge of the downstream cavity trench. On the other hand, the experimentally measured partial loss (experiment) excludes some of the profile and endwall losses near the blade surfaces and hub endwall due to the finite size of the probe. Figure 8 also shows the numerically calculated losses corresponding to the measured points $\mathrm{CFD}_{\mathrm{partial}}$, and the corresponding numerical and experimental loss trends are similar. From the blade LE ($x/C_x = 0.0$) up to the midchord ($x/C_x = 0.5$), the loss concentrated near the hub endwall and blade surfaces seems to cause approximately 23% of the total loss, whereas

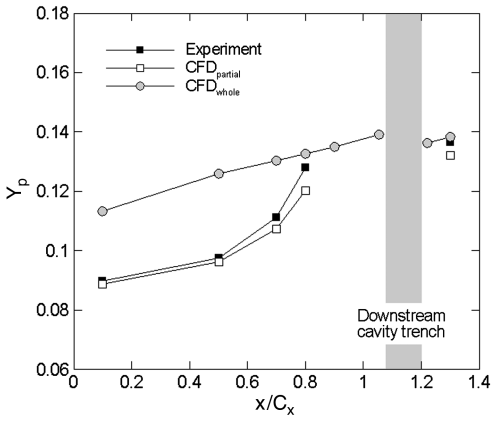

Fig. 8 Streamwise evolution of measured and numerically simulated loss at four selected axial chordwise locations for the design point, $v_y/U_{\mathrm{hub}} = 0.35$.

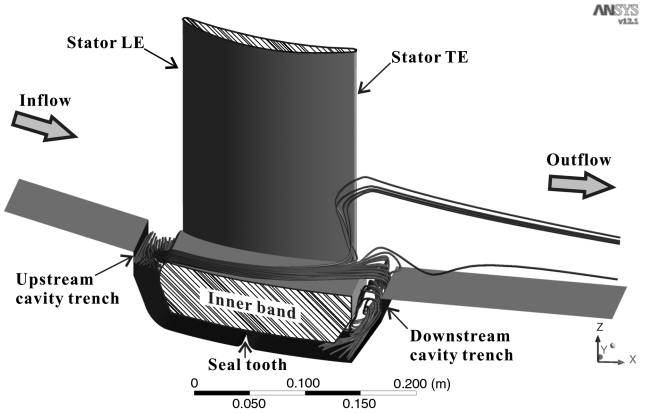

Fig. 9 Simulated streamline of injected high-loss fluids from the upstream cavity trench in the blade passage for the design point, $v_y/U_{\text{hub}} = 0.35$.

its contribution is about 4% of the total loss at $x/C_x = 0.8$. At $x/C_x = 1.3$, the probe captures the wake region as well; therefore, the agreement among experimental, $\text{CFD}_{\text{whole}}$, and $\text{CFD}_{\text{partial}}$ losses is better.

Still farther downstream, between $x/C_x = 1.0$ and 1.2, the total loss $\text{CFD}_{\text{whole}}$ decreases. This decrease in the total loss is due to the ingestion of the high-loss fluids through the downstream cavity trench. At the downstream cavity trench, the mainstream flow near the hub is engulfed into the seal cavity and rejoins the mainstream flow via the upstream cavity trench, due to the adverse pressure gradient in the axial direction (see Fig. 9). Heidegger et al. [5] and Wellborn [19] suggested that a majority of the low momentum fluids are ingested into the downstream cavity. At $x/C_x = 1.3$, the loss again begins to increase due to the stator blade wakes and mixing effects.

V. Conclusions

Conclusions of this study are summarized as follows:

1) To simulate the effects of rotation in a shrouded compressor linear cascade, a secondary flow loop for the seal cavity leakage flow has been added. The results show that the overall loss and deviation are qualitatively and quantitatively comparable to the data from rotating conditions.

2) In the blade passage, the low momentum fluids continuously move toward the blade suction side near the hub endwall due to the cross-passage pressure gradient, resulting in a high-loss region in the hub suction side corner.

3) After successively increasing up to the upstream edge of the downstream cavity trench, the loss is decreased due to the ingestion of high-loss fluids into the seal cavity via the downstream cavity trench.

4) Downstream of the downstream cavity at $x/C_x = 1.3$, the loss again begins to increase, mainly due to the wakes shed from the blades.

Acknowledgments

The authors would like to acknowledge support from the BK21 program and the Institute of Advanced Machinery and Design at Seoul National University. The authors are also grateful to H. W. Shin and D. C. Wisler of GE Aircraft Engines for their advice regarding the shrouded axial compressor stator geometry.

References

[1] Wisler, D. C., "Loss Reduction in Axial-Flow Compressors Through Low-Speed Model Testing," *Journal of Engineering for Gas Turbines and Power*, Vol. 107, No. 2, April 1985, pp. 354–363. doi:10.1115/1.3239730

[2] Wisler, D. C., Bauer, R. C., and Okiishi, T. H., "Secondary Flow, Turbulent Diffusion, and Mixing in Axial-Flow Compressors," *Journal of Turbomachinery*, Vol. 109, No. 4, Oct. 1987, pp. 455–482. doi:10.1115/1.3262127

[3] Wellborn, S. R., and Okiishi, T. H., "Effects of Shrouded Stator Cavity Flows on Multistage Axial Compressor Aerodynamic Performance," NASA CR 198536, 1996.

[4] Wellborn, S. R., and Okiishi, T. H., "The Influence of Shrouded Stator Cavity Flows on Multistage Compressor Performance," *Journal of Turbomachinery*, Vol. 121, No. 3, July 1999, pp. 486–498. doi:10.1115/1.2841341

[5] Heidegger, N. J., Hall, E. J., and Delaney, R. A., "Parameterized Study of High-Speed Compressor Seal Cavity Flow," AIAA Paper 1996-2807, 1996.

[6] Yaras, M. I., and Sjolander, S. A., "Effects of Simulated Rotation on Tip Leakage in a Planar Cascade of Turbine Blades. Part 1: Tip Gap Flow," *Journal of Turbomachinery*, Vol. 114, No. 3, July 1992, pp. 652–659. doi:10.1115/1.2929189

[7] Yaras, M. I., Sjolander, S. A., and Kind, R. J., "Effects of Simulated Rotation on Tip Leakage in a Planar Cascade of Turbine Blades. Part 2: Downstream Flow Field and Blade Loading," *Journal of Turbomachinery*, Vol. 114, No. 3, July 1992, pp. 660–667. doi:10.1115/1.2929190

[8] Palafox, P., Oldfield, M. L. G., LaGraff, J. E., and Jones, T. V., "PIV Maps of Tip Leakage and Secondary Flow Fields on a Low-Speed Turbine Blade Cascade With Moving End Wall," *Journal of Turbomachinery*, Vol. 130, No. 1, Jan. 2008, Paper 011001. doi:10.1115/1.2437218

[9] Krishnababu, S. K., Dawes, W. N., Hodson, H. P., Lock, G. D., Hannis, J., and Whitney, C., "Aerothermal Investigations of Tip Leakage Flow in Axial Flow Turbines, Part 2: Effect of Relative Casing Motion," *Journal of Turbomachinery*, Vol. 131, No. 1, Jan. 2009, Paper 011007. doi:10.1115/1.2952378

[10] Demargne, A. A. J., and Longley, J. P., "Aerodynamic Interaction of Stator Shroud Leakage and Mainstream Flows in Compressors," American Soc. of Mechanical Engineers Paper 2000-GT-570, New York, 2000.

[11] de la Rosa Blanco, E., Hodson, H. P., and Vazquez, R., "Effect of the Leakage Flows and the Upstream Platform Geometry on the Endwall Flows of a Turbine Cascade," *Journal of Turbomachinery*, Vol. 131, No. 1, Jan. 2009, Paper 011004. doi:10.1115/1.2950052

[12] Sohn, D. W., Kim, T., and Song, S. J., "Effects of Leakage Flow Tangential Velocity on Leakage Flow Path in Shrouded Axial Compressor Cascades," *Asian Congress of Gas Turbine (ACGT)*, ACGT Paper 015, Seoul, 2005.

[13] Lee, J. S., "Effects of the Shrouded Cavity on Loss in Axial Compressor Cascade," M.S. Thesis, School of Mechanical and Aerospace Engineering, Seoul National Univ., Seoul, 2005.

[14] Sohn, D. W., Kim, T., and Song, S. J., "Influence of Leakage Tangential Velocity on Leakage Flow Path and Passage Flow in Shrouded Axial Compressor Cascades," International Symposium on Transport Phenomena and Dynamics of Rotating Machinery (ISROMAC), ISROMAC-11 Paper 73, 2006.

[15] Wisler, D. C., "Core Compressor Exit Stage Study: Vol. 1, Blading Design," NASA CR 135391, 1977.

[16] Coleman, H. W., and Steele, W. G., *Experimentation and Uncertainty Analysis for Engineers*, 2nd ed., Wiley, New York, 1999, pp. 40–74.

[17] Wisler, D. C., "Core Compressor Exit Stage Study: Vol. 2, Data and Performance Report for the Baseline Configuration," NASA CR 159498, 1980.

[18] Gbadebo, S. A., Cumpsty, N. A., and Hynes, T. P., "Three-Dimensional Separations in Axial Compressors," *Journal of Turbomachinery*, Vol. 127, No. 2, April 2005, pp. 331–339. doi:10.1115/1.1811093

[19] Wellborn, S. R., "Details of Axial Compressor Shrouded Stator Cavity Flows," American Soc. of Mechanical Engineers Paper 2001-GT-0495, New York, 2001.

R. Miller
Associate Editor